Inorganica Chimica Acta, 33 (1979) 215–225
©Elsevier Sequoia S A , Lausanne – Printed in Switzerland

Photochemistry of $Cr(CO)_5PCl_3$, $Cr(CO)_5$pyridine and $Cr(CO)_5$pyrazine in Ar matrices at 10 K.
Evidence for the Formation of $Cr(CO)_5$ and Two Novel Complexes *cis*-$Cr(CO)_4$-pyridine and *cis*-$Cr(CO)_4$pyrazine

G BOXHOORN D J STUFKENS and A OSKAM*

Anorganisch Chemisch Laboratorium, University of Amsterdam, J H van't Hoff Instituut, Nieuwe Achtergracht 166, 1018 WV Amsterdam, The Netherlands

Received September 7, 1978

Photolysis of $Cr(CO)_5PCl_3$ in an Ar matrix at 10 K with different wavelengths (λ = 229, 254, 280, 313 and 366 nm) resulted in the formation of $Cr(CO)_5$ The reaction is reversed by irradiation with λ = 546 nm Photolysis of $Cr(CO)_5$ pyridine and $Cr(CO)_5$-pyrazine in an Ar matrix at 10 K generated CO or the unique ligand, depending on the irradiated wavelength New five coordinated species were detected cis-*$Cr(CO)_4$pyridine and* cis-*$Cr(CO)_4$pyrazine Regeneration of the parent compound was only partly accomplished due to formation of* trans-*$Cr(CO)_4$pyridine and -$Cr(CO)_4$pyrazine The difference in photochemical behaviour between PCl_3 and nitrogen donor ligand complexes is discussed with the use of a m o scheme Infrared and UV–visible data are reported in various media and assigned*

Introduction

During the last few years the photolability of substituted Group VI carbonyls has been studied [1–7] The photochemistry of $M(CO)_5L$ complexes involves CO or unique ligand substitution, depending on the type of ligand, the central metal atom and on the irradiated wavelength

$$M(CO)_5L \xrightarrow[X]{h\nu} M(CO)_4LX + CO$$

$$M(CO)_5L \xrightarrow[X]{h\nu'} M(CO)_5X + L$$

X = ligand or vacancy in matrices

Quantum yield studies of $M(CO)_5$amine (M = Mo and W) [1–3] have shown that M–L bond cleavage is far more favourable than M–C bond cleavage, although CO substitution becomes more important at shorter wavelength irradiation The same conclusions were drawn by Dahlgren and Zink [5] For phosphorus-donor complexes $W(CO)_5L$ (L = PPh_3, PBr_3, PCl_3, PH_3, $P(n\text{-}Bu)_3$) they found however, that efficient carbon monoxide and unique ligand substitution can both occur Recently, ligand photosubstitution chemistry of $Mo(CO)_5PPh_3$ has demonstrated that CO substitution dominates at λ = 366 nm (ϕ_{366} = 0 58) with lower quantum efficiency for unique ligand loss (ϕ_{366} = 0 11) Formation of *cis*- and *trans*-$Mo(CO)_4PPh_3L$ complexes in the presence of L and photoisomerization of the *trans*-isomer into the *cis*-complex was observed [6] In the course of our investigations Darensbourg and Murphy reported for the first time that for chromium derivatives in contrast to molybdenum and tungsten, the M–C bond dissociation at 313 and 366 nm is equally or more important than M–N cleavage [7] In solution photochemistry it is very difficult to deduce which intermediates are involved Matrix isolation spectroscopy, however, has shown to be a powerful tool in resolving structures of unstable transition metal carbonyl complexes [8–12] About the photochemistry of substituted carbonyls studied with matrix isolation spectroscopy only a few articles have been published [13–18] Poliakoff reported the UV photolysis of $M(CO)_5CS$ (M = Cr or W) in several matrices [13, 14] Evidence was found for the formation of both *cis*- and *trans*-$M(CO)_4CS$ after photolysis with λ = 300 nm The reaction was reversed after long periods of irradiation with unfiltered visible light No evidence was found for loss of CS In a hydrocarbon glass Black obtained similar results with $Mo(CO)_5P(C_6H_{11})_3$ [15] Rest described the photochemistry of $W(CO)_5L$ (L = pyridine, 3-bromopyridine or hydrogen sulfide) in several matrices at 10 K with 320 < λ < 390 nm which resulted in the formation of $W(CO)_5$ [16, 17] This indicates for the first time that also bulky ligands can be generated in a matrix The reaction was reversed by subsequent irradiation with visible light

---

*To whom correspondence should be addressed

The same results were found for $W(CO)_5PCl_3$ in an Ar matrix at 10K, as we reported in an earlier paper [18]. Photodetachment of PCl_3 was found by irradiation with λ = 229, 254, 280, 313 and 366 nm. Recoordination of PCl_3 was accomplished by long wavelength irradiation with λ = 436 nm.

In this article we report the photochemistry of $Cr(CO)_5L$ derivatives, in which L = PCl_3, pyridine and pyrazine, in an Ar matrix at 10K. For the first time evidence will be presented of both CO and unique ligand rupture for the same complex in a matrix, depending on the ligand and on the irradiated wavelength. New sixteen electron species *cis*-$Cr(CO)_4$ pyridine and *cis*-$Cr(CO)_4$pyrazine will be described. The reactions were only partly photochromic due to the formation of *trans*-$Cr(CO)_4N$ donor complexes. Preliminary results for $Cr(CO)_5PCl_3$ and $Cr(CO)_5$-pyrazine have previously been reported by us [19].

Experimental

The chromium complexes were prepared from the corresponding $Cr(CO)_5THF$ complex under a stream of dry nitrogen, as has been published by Strohmeier [20]. After evaporation of THF, impurities of unreacted $Cr(CO)_6$ were removed by vacuum sublimation at room temperature. Recrystallization from n-hexane and high vacuum sublimation at about 50 °C resulted in pure $Cr(CO)_5L$ complexes [21, 22].

The equipment used to achieve cryogenic temperatures, an Air Products Displex model CSW-202 B closed cycle helium refrigerator, has been described in detail before [18]. The sample window of CsBr or CsI had a temperature of 10K during deposition and the vacuum was better than 10^{-6} torr. Gas mixtures of $Cr(CO)_5PCl_3$ and Ar (purity 99.999%) were made by adding Ar to the vapour of the sample [23]. The best results were obtained with a gas mixture of 1:5200 and the pulse technique of Rochkind [24, 25]. For $Cr(CO)_5$pyridine and $Cr(CO)_5$pyrazine possessing low vapour pressures, an oven was built. Oven temperature never exceeded 40 °C, since an extensive increase of decomposition into $Cr(CO)_6$ was detected above this temperature. Deposition times varied between one and two hours, using the slow spray-on technique.

Infrared spectra were recorded on Beckman IR-7, IR-11, IR-12 and IR-4250 spectrometers. The resolution was better than 0.8 cm^{-1} in the CO stretching region and varied between 3.6 and 0.7 cm^{-1} in the region below 700 cm^{-1}. Vapour phase spectra were recorded using a Beckman 10 meter multipath gas cell.

UV–visible absorption spectra were recorded on a Cary 14 spectrophotometer with an extended sample compartment and optical density screens in the reference beam. CsBr and CsI sample windows were replaced by a NaCl window in order to avoid UV absorptions in the region between 200 and 230 nm.

Photolysis was carried out with a Philips 25W Cd-line source, model 93107 and a Philips HPK 125W high pressure Hg lamp. The light of this latter lamp was filtered using interference filters for λ = 254, 280, 313, 334, 366, 405 nm from Meyvis and λ = 436 and 546 nm from Balzers. The heat from the lamp was removed by a quartz water cell of 5 cm.

Results

IR Spectra

The IR spectra of $M(CO)_5L$ molecules in the CO stretching region have been studied extensively [26–28]. For the $M(CO)_5$ moiety with local symmetry C_{4v} three CO vibrations are expected: $2A_1 + E$, although the formally infrared inactive B_1 mode has also been observed. The infrared spectra are presented in the Figures 1, 2 and 3.

The spectra nicely show the shift of the A_1^1 (*trans*) vibration going from PCl_3 to pyrazine and pyridine, which was anticipated. Matrix splittings were measured for most bands, although for the nitrogen donor complexes considerably more splittings were observed, especially for $Cr(CO)_5$pyridine. These splittings are due to different sites of the same molecule trapped in the matrix, although the reason why $Cr(CO)_5$pyridine has more splittings is not clear.

Thermal decomposition of the nitrogen ligand complexes could not be avoided because CO stretching modes of $Cr(CO)_6$ were detected as has been published before [17, 19].

The low frequency region is more difficult to assign and only a few articles have been published [29–31]. For the $M(CO)_5$ moiety four infrared active δ(M–C–O), (A_1 + 3E) and three ν(M–C), ($2A_1$ + E) vibrations are expected. Not all δ(M–C–O) deformations were found, since two of the bands always have a very low intensity. For $M(CO)_5PCl_3$ molecules, the infrared spectra of $Mo(CO)_5PCl_3$ and $W(CO)_5PCl_3$ have completely been assigned before [18, 22]. Assignments, however, for $Cr(CO)_5PCl_3$ were only possible with the aid of Raman spectra. A ν(P–Cl) was found at 511 cm^{-1}. A band between 310 and 300 cm^{-1} was tentatively assigned to ν(Cr–P). A study of the infrared and Raman spectra of $M(CO)_5$-PX_3 molecules (M = Cr, Mo, W; X = F, Cl, Br, Ph) must resolve the problem of the assignment of ν(M–P) [32]. δ(Cr–C–O) and ν(Cr–C) of $Cr(CO)_5$-pyridine and $Cr(CO)_5$pyrazine were assigned according to Young and Daamen [29, 33].

Ligand vibrations of pyridine and pyrazine were not measured because these modes could only be observed for large amounts of deposited samples.

TABLE I. Infrared Frequencies of $Cr(CO)_5PCl_3$ in cm^{-1}.

Assignments	νC–O				$\nu\ ^{13}$C–O	δCr–C–O			νPCl	νCr–C			
	A_1^2	B_1	A_1^1	E	E	A_1	E	E		A_1^1	E	B_1	A_1^2
$Cr(CO)_5PCl_3$ nujol mull, RT	2085.4	[b]	1999.8	1982.1	1952.1	657	647	534	515	455	433	406	386
$Cr(CO)_5PCl_3$ n-heptane, RT	2088.4	2022.2	2000.8	1984.0	1952.6	658	647	531	508	453	430	406	386
$Cr(CO)_5PCl_3$ Ar matrix, 10K	2093.6	2024.3	2005.9	1990.9 1987.0[a]	1958.6	662	651	533	511	458	433	408	390
Band number	1	2	3	4	5	6	7	8	9	10	11	12	13
$Cr(CO)_5PCl_3$ gas phase, RT	2094.9	[b]	2012.2	1997.5	1965.5	661	653	535	519	454	431	407	387
Intensity	W	W	M	S	W	S	S	W	S	W	S	W	M

[a] Most intense band. [b] Not observed.

TABLE II. Infrared Frequencies of $Cr(CO)_5$pyridine in cm^{-1}.

Assignments	νC–O				$\nu\ ^{13}$C–O	δCr–C–O			νCr–C			
	A_1^2	B_1	E	A_1^1	E	A_1	E	E	A_1^1	E	B_1	A_1^2
$Cr(CO)_5$pyridine nujol mull, RT	2064.6	1972.3	1936.7[a] 1917.6	1894.8	[b]	660	649	550	476	441	413	397
$Cr(CO)_5$pyridine n-hexane, RT	2068.7	[b]	1938.7	1920.5	1895.5	669	654	b	473	441	423	400
$Cr(CO)_5$pyridine Ar matrix, 10K	2072.5	1982.2	1953.7 1943.5[a] 1938.7 1930.4	1923.9	1902.5	676	660	554	[b]	445	426	403
Band number	1	2	3	4	5	6	7	8		9	10	11
Intensity	W	W	S	M	W	S	S	W	W	S	W	M

[a] Most intense band. [b] Not observed.

TABLE III. Infrared Frequencies of $Cr(CO)_5$pyrazine in cm^{-1}.

Assignments	νC–O			$\nu\ ^{13}$C–O	δCr–C–O			νCr–C			
	A_1^2	E	A_1^1	E	A_1	E	E	A_1^1	E	B_1	A_1^2
$Cr(CO)_5$pyrazine nujol mull, RT	2068.6	1940.0	1879.8	1843.2	666	652	554	473	438	[b]	407
$Cr(CO)_5$pyrazine n-hexane, RT	2069.3	1944.0	1929.9	1912.6	665	653	551	b	437	415	402
$Cr(CO)_5$pyrazine Ar matrix, 10K	2074.0	1958.8 1951.5 1947.8[a] 1942.9	1933.8	1912.9	671	657	548	474(sh)	444	428	400
Band number	1	2	3	4	5	6	7	8	9	10	11
Intensity	W	S	M	W	S	S	W	W	S	W	M

[a] Most intense band. [b] Not observed.

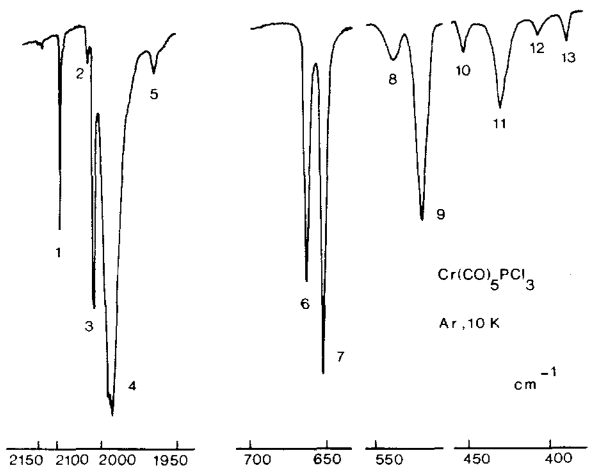

Figure 1. Infrared spectra of Cr(CO)$_5$PCl$_3$ in an Ar matrix at 10K, after deposition with the pulse technique, S/M = 1/5200 (below 700 cm^{-1} the spectrum was recorded with ordinate scale expansion).

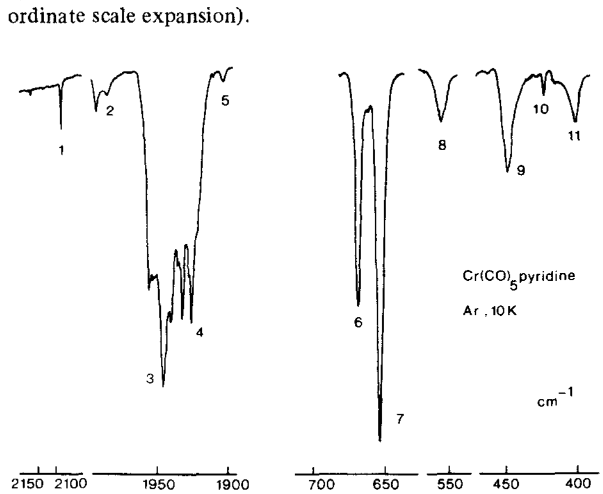

Figure 2. Infrared spectrum of Cr(CO)$_5$pyridine in an Ar matrix at 10K, after codeposition (below 700 cm^{-1} the spectrum was recorded with ordinate scale expansion).

In Tables I, II and III the influence of various media (nujol mull, n-hexane, Ar matrix, gas phase) is demonstrated.

UV–Visible Spectra

In Figures 4, 5 and 6 the UV–Visible absorption spectra of Cr(CO)$_5$PCl$_3$, Cr(CO)$_5$pyridine and Cr(CO)$_5$pyrazine in an Ar matrix at 10 K are presented. In the Cr(CO)$_5$PCl$_3$ spectrum four bands could be distinguished: two Cr(3d) → π*CO CT bands, one Cr(3d) → π^*(PCl$_3$) CT band and one LF band, from which the latter is assigned to the orbital and spin allowed $^1E(b_2^2e^3a_1^1) \rightarrow {}^1A_1(b_2^2e^4)$ transition. The assignments are in agreement with those for Mo(CO)$_5$PCl$_3$ and W(CO)$_5$PCl$_3$ [18, 27].

The nitrogen donor complexes have a very intense Cr(3d) → π^*CO CT band which obscures the second Cr(3d) → π^*CO band between 280 and 290 nm.

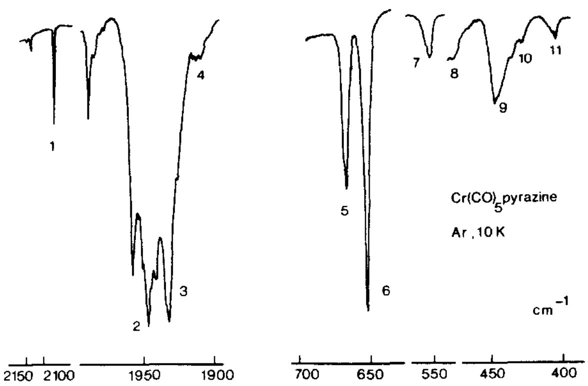

Figure 3. Infrared spectrum of Cr(CO)$_5$pyrazine in an Ar matrix at 10K, after codeposition (below 700 cm^{-1} the spectrum was recorded with ordinate scale expansion).

Apart from these bands one LF transition at 405 nm was detected for Cr(CO)$_5$pyrazine and two at 327 and 412 nm respectively for Cr(CO)$_5$pyridine. The band at 327 nm is assigned to the orbital, spin allowed $^1E(b_2^2e^3b_1^1) \leftarrow {}^1A_1(b_2^2e^4)$ and/or the orbital forbidden, spin allowed $^1A_2(b_2^1e^4b_1^1) \leftarrow {}^1A_1(b_2^2e^4)$ transition [2, 7] and the band at about 417 nm to the orbital and spin allowed $^1E(b_2^2e^3a_1^1) \leftarrow {}^1A_1(b_2^2e^4)$ transition in agreement with the LF transitions found in a series of M(CO)$_5$ N-donor complexes [21]. Solvatochromic Cr(3d) → π^*(pyridine) and Cr(3d) → π^*(pyrazine) transitions were found at 361 and 405 nm respectively. These MLCT bands were, in contrast to LF transitions, blue shifted with increasing polarity of the solvent, due to a strong interaction of π^* ligand orbitals with the solvent [21, 31]. Surprisingly, going from n-hexane to an Ar matrix these MLCT bands are also blue shifted: for Cr(CO)$_5$-pyridine a shift from about 387 to 361 nm was detected. In Cr(CO)$_5$pyrazine, the MLCT band shifts from about 453 to 405 nm and coincides with the LF transition.

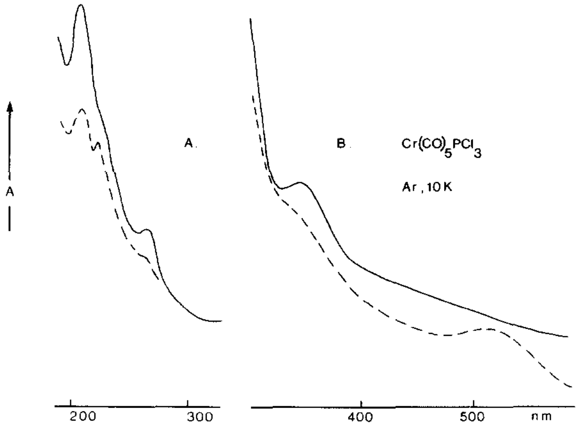

Figure 4. A. UV–Visible absorption spectrum of Cr(CO)$_5$-PCl$_3$ in an Ar matrix at 10K. B. Spectrum after a long deposition time: (——) before photolysis, (------) after 1020 min photolysis with λ = 313 nm.

TABLE IV. UV-Visible Absorption Bands of $M(CO)_5L$ (in nm).

Assignments	$d \rightarrow \pi^*(CO)$	$d \rightarrow \pi^*(CO)$	$d \rightarrow \pi^*(L)$	$d \rightarrow d$	$d \rightarrow d$	Intraligand
$Cr(CO)_5PCl_3$ n-hexane, RT	227	287	252	–	362	–
$Cr(CO)_5PCl_3$ Ar matrix, 10K	224	282	247	–	362	–
$Cr(CO)_5$pyridine n-hexane, RT	231	~280	387[a]	336	387[a]	–
$Cr(CO)_5$pyridine Ar matrix, 10K	235	~280	361	327	412	–
$Cr(CO)_5$pyrazine n-hexane, RT	244	~290	453	–	422	320–330
$Cr(CO)_5$pyrazine Ar matrix, 10K	240	~285	405[a]	–	405[a]	310–330

[a] Coinciding bands.

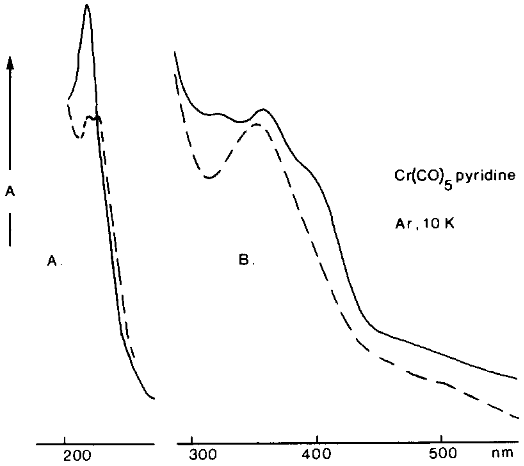

Figure 5. A. UV–Visible absorption spectrum of $Cr(CO)_5$ pyridine in an Ar matrix at 10K. B. Spectrum after a long deposition time: (———) before photolysis, (------) after 1020 min photolysis with λ = 313 nm.

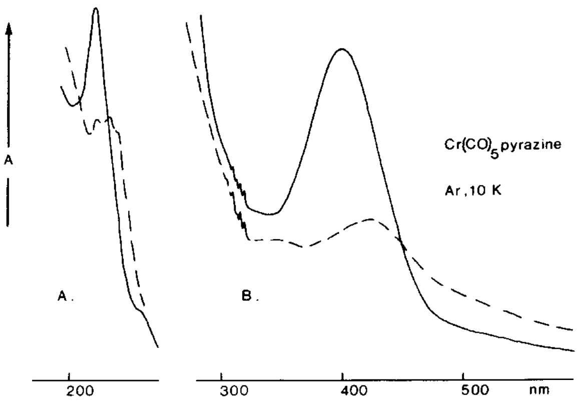

Figure 6. A. UV–Visible absorption spectrum of $Cr(CO)_5$ pyrazine in an Ar matrix at 10K. B. Spectrum after a long deposition time: (———) before photolysis, (------) after 170 min photolysis with λ = 229 nm.

In the region between 310 and 330 nm intraligand transitions of pyrazine were observed. Going from $Cr(CO)_5PCl_3$ to $Cr(CO)_5$pyridine and $Cr(CO)_5$ pyrazine a shift of the lowest energy (LF) transition is observed, which is caused by a decrease of π backbonding, when PCl_3 is replaced by pyridine or pyrazine.

In Table IV the influence on the spectra going from an Ar matrix to n-hexane is presented.

Photochemistry

Photolysis of $Cr(CO)_5PCl_3$

Irradiation of $Cr(CO)_5PCl_3$ in an Ar matrix at 10K with monochromatic light (λ = 229, 254, 280, 313 and 366 nm) produced after a few minutes two new infrared bands at 1965 and 1935 cm^{-1} which are similar to those observed by Turner and assigned to the E and A_1 modes of the $Cr(CO)_5$ fragment [8]. Although for $Cr(CO)_5$ with symmetry C_{4v}, three bands are expected, the third one at 2093 cm^{-1} is only observed for high concentrations of $Cr(CO)_5$. Besides $Cr(CO)_5$, free PCl_3 was detected from a band at 500 cm^{-1}. The UV–visible spectra showed two new absorption bands at 237 and 540 nm, due to a Cr → π^*CO and a LF transition of $Cr(CO)_5$, respectively.

After prolonged photolysis, even $Cr(CO)_4$ and free CO were detected*. The product bands disappeared

---

*Besides $Cr(CO)_4$ sometimes a weak band at 1948 cm^{-1} was detected, which is tentatively assigned to small amounts of *trans*-$Cr(CO)_4PCl_3$.

after irradiation in the visible absorption band of $\mathrm{Cr(CO)_5}$ with λ = 436 or λ = 546 nm. Similar photochemical behaviour has been found for $\mathrm{Cr(CO)_6}$ and $\mathrm{W(CO)_5PCl_3}$ [8, 18]. This photolysis of $\mathrm{Cr(CO)_5PCl_3}$ which appeared to be independent of the wavelength, is shown in Fig. 7.

$$\mathrm{Cr(CO)_5PCl_3} \underset{\lambda = 436,\ 546}{\overset{\lambda \leqslant 366}{\rightleftharpoons}} \mathrm{Cr(CO)_5} + \mathrm{PCl_3}$$

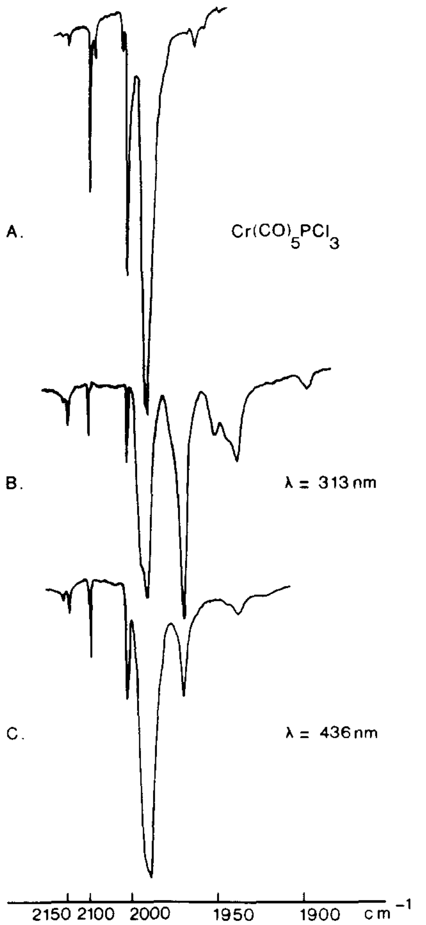

Figure 7. Infrared spectrum of $\mathrm{Cr(CO)_5PCl_3}$ in an Ar matrix at 10 K. A. After deposition. B. After 960 min photolysis with λ = 313 nm. C. After 120 min photolysis with λ = 436 nm.

Photolysis of Cr(CO)₅pyridine

The photochemistry of $\mathrm{Cr(CO)_5}$pyridine is different from that of $\mathrm{Cr(CO)_5PCl_3}$. By irradiation with λ = 229, 254, 280, 313 nm the parent bands decreased and totally new frequencies appeared at 2032, 1916, 1908 and 1885 $\mathrm{cm^{-1}}$* together with a band at 2138 $\mathrm{cm^{-1}}$ from free CO. Comparing these bands with those found for *cis*-$\mathrm{Cr(CO)_4CS}$ and *cis*-$\mathrm{Mo(CO)_4P(C_6H_{11})_3}$, we attribute these frequencies to the new sixteen electron species *cis*-$\mathrm{Cr(CO)_4}$pyridine with $\mathrm{C_s}$ symmetry [13, 15]. At the same time the band in the absorption spectra at 235 nm shifted to 240 nm while a new band appeared at 351 nm, which we will discuss below. The formation of *cis*-$\mathrm{Cr(CO)_4}$pyridine is related to the formation of *cis*-$\mathrm{Cr(CO)_4{}^{13}CO}$pyridine in solution photochemistry, formed by irradiation with λ = 313 and 366 nm in the presence of $\mathrm{^{13}CO}$ [6].

After extended irradiation time new bands were observed with frequencies 1851 and 1836 $\mathrm{cm^{-1}}$, closely related to *fac*-$\mathrm{Mo(CO)_3P(C_6H_{11})_3}$ with local $\mathrm{C_{3v}}$ symmetry [15]. The bands are tentatively assigned to the *fac* isomer of $\mathrm{Cr(CO)_3}$pyridine with two vacant coordination sites.

When *cis*-$\mathrm{Cr(CO)_4}$pyridine was formed, less intensive bands of $\mathrm{Cr(CO)_5}$ were detected. The formation of $\mathrm{Cr(CO)_5}$ was strongly dependent on the irradiated wavelength. In the series λ = 229, 254, 280, 313, 334, 366, 405, 436 nm, the ratio $\mathrm{Cr(CO)_5}$/*cis*-$\mathrm{Cr(CO)_4}$pyridine increased and was greater than unity at the wavelengths 334, 366, 405 and 436 nm. Therefore, the "turning point" is located between 313 and 334 nm.

The reactions showed to be photochromic, but not totally: photolysis with λ = 546 nm destroyed both $\mathrm{Cr(CO)_5}$ and *cis*-$\mathrm{Cr(CO)_4}$pyridine, while large amounts of $\mathrm{Cr(CO)_5}$pyridine were regenerated. Besides this, a new infrared band appeared at 1907.9 $\mathrm{cm^{-1}}$, which was assigned to *trans*-$\mathrm{Cr(CO)_4}$pyridine. This latter band was not found when $\mathrm{Cr(CO)_5}$pyridine was photolyzed with λ = 546 nm for a long period. When all $\mathrm{Cr(CO)_5}$ or *cis*-$\mathrm{Cr(CO)_4}$pyridine fragments had disappeared, no enhancement of the 1907.9 $\mathrm{cm^{-1}}$ band was detected any more, indicating that *trans*-$\mathrm{Cr(CO)_4}$pyridine originated from either $\mathrm{Cr(CO)_5}$ or *cis*-$\mathrm{(CO)_4}$pyridine as we will discuss.

$$\begin{tikzcd}
\mathrm{Cr(CO)_5pyridine} \arrow[r, shift left, "\lambda \leqslant 313"] & \mathit{cis}\text{-}\mathrm{Cr(CO)_4pyridine} + \arrow[l, shift left] \arrow[d, "\lambda = 546"] \\
\mathrm{CO}(+\mathrm{Cr(CO)_5}) & \mathit{trans}\text{-}\mathrm{Cr(CO)_4pyridine}
\end{tikzcd}$$

$$\begin{tikzcd}
\mathrm{Cr(CO)_5pyridine} \arrow[r, shift left, "\lambda \geqslant 334"] & \mathrm{Cr(CO)_5} + \mathrm{pyridine}\text{-} \arrow[l, shift left] \arrow[d, "\lambda = 546"] \\
(+\mathit{cis}\text{-}\mathrm{Cr(CO)_4pyridine})\text{-} & \mathit{trans}\text{-}\mathrm{Cr(CO)_4pyridine}
\end{tikzcd}$$

This photochemical behaviour is shown in Figures 8 and 9.

Photolysis of Cr(CO)₅pyrazine

The photochemical behaviour of $\mathrm{Cr(CO)_5}$pyrazine is the same as found for $\mathrm{Cr(CO)_5}$pyridine. *Cis*-$\mathrm{Cr(CO)_4}$pyrazine was the main product by irradiation with the wavelengths 229, 254, 280 and 313 nm and $\mathrm{Cr(CO)_5}$ by irradiation with λ = 405 and 436 nm. Observed infrared frequencies for *cis*-$\mathrm{Cr(CO)_4}$-

---

*Split band.

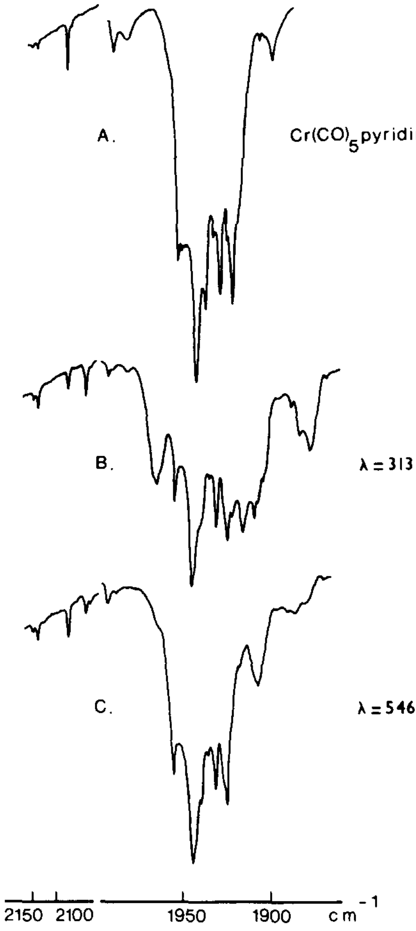

Figure 8. Infrared spectrum of Cr(CO)$_5$pyridine in an Ar matrix at 10 K. A. After deposition. B. After 960 min photolysis with λ = 313 nm. C. After 80 min photolysis with λ = 546 nm.

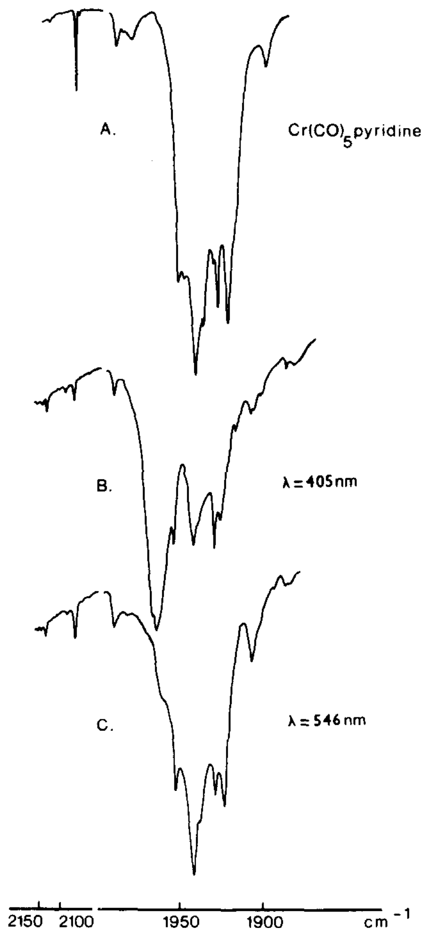

Figure 9. Infrared spectrum of Cr(CO)$_5$pyridine in an Ar matrix at 10 K. A. After deposition. B. After 150 min photolysis with λ = 405 nm. C. After 90 min photolysis with λ = 546 nm.

pyrazine were 2037, 1927*, 1915*, 1884* cm^{-1}. UV–Visible absorptions were found at 254, 261(sh), 353 and 432 nm. The difference between LF transitions of *cis*-Cr(CO)$_4$pyridine and *cis*-Cr(CO)$_4$pyrazine will be small. We therefore assign the respective bands at 351 and 353 nm of these complexes to the same LF transition (Fig. 5 and 6). The Cr(3d) → π* (pyrazine) CT transition in *cis*-Cr(CO)$_4$pyrazine is found at 432 nm. In agreement with the corresponding pentacarbonyls (Table IV, Fig. 5 and 6) this MLCT transition is expected at higher energy for *cis*-Cr(CO)$_4$pyridine; it will coincide with the LF transition at 351 nm. Lower lying LF transitions, as have been found for *cis*-Cr(CO)$_4$CS, were not detected, although it is possible that they are obscured by the LF transition of Cr(CO)$_5$ in the visible region.

The formation of *cis*-Cr(CO)$_4$pyrazine was partly reversed by irradiation with λ = 546 nm; a new IR band at 1910 cm^{-1} was attributed to the formation of *trans*-Cr(CO)$_4$pyridine. The "reversal" Cr(CO)$_5$+ pyrazine → Cr(CO)$_5$pyrazine was also detected by irradiation with λ = 229 nm, but in that case no growth of parent bands was observed, due to rapid decomposition of Cr(CO)$_5$pyrazine into *cis*-Cr(CO)$_4$-pyrazine.

The same results were obtained when after photolyzing with λ = 229 nm the reaction was "reversed" with λ = 405 nm, causing growth of the Cr(CO)$_5$ frequencies. Warming the matrix to 30K, the bands of Cr(CO)$_5$ and *cis*-Cr(CO)$_4$pyrazine decreased simultaneously and new Cr(CO)$_5$pyrazine was formed. The presence of small amounts of Cr(CO)$_6$, during the investigations with Cr(CO)$_5$pyridine and Cr(CO)$_5$pyrazine had very little influence on the photochemical reactions. After extended irradiation time *fac*-Cr(CO)$_3$pyrazine was detected at 1863 and 1843 cm^{-1}. The infrared spectra are shown in Figures 10 and 11 and the infrared frequencies of 16-electron fragments are tabulated in Table V.

---

*Split bands.

TABLE V. Infrared Frequencies of 16 Electron $Cr(CO)_5$, *cis*-$Cr(CO)_4$pyridine and *cis*-$Cr(CO)_4$pyrazine in cm^{-1} (Ar matrix).

Assignments	ν C–O						
	A_1	A′	E	A_1	A′	A″	A′
$Cr(CO)_5$...Ar	2092.9		1965.1	1935.1[a]	–	–	–
cis-pyridine$Cr(CO)_4$...Ar	–	2032.3	–	–	1915.9	1907.8	1884.6 1878.3
cis-pyrazine$Cr(CO)_4$...Ar	–	2036.5	–	–	1927.3 1922.8	1914.5 1909.9	1889.9 1884.2

[a] Obscured by parent bands in $Cr(CO)_5$pyridine and $Cr(CO)_5$pyrazine.

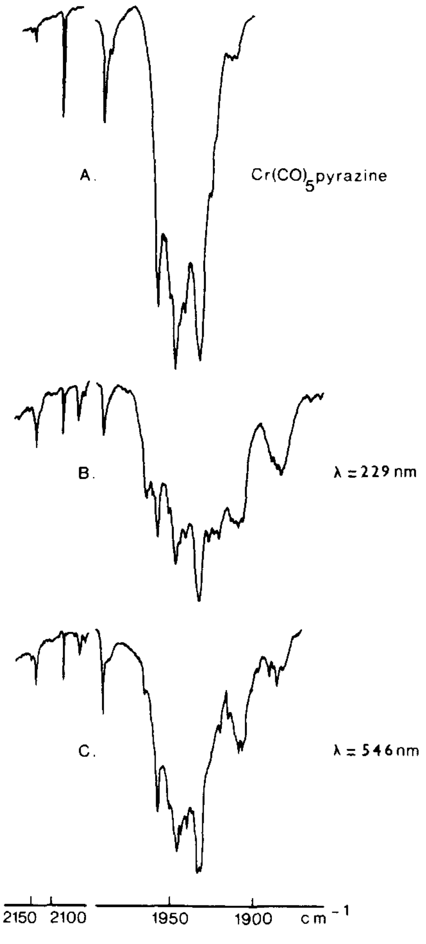

Figure 10. Infrared spectrum of $Cr(CO)_5$pyrazine in an Ar matrix at 10 K. A. After deposition. B. After 180 min photolysis with λ = 229 nm. C. After 110 min photolysis with λ = 546 nm.

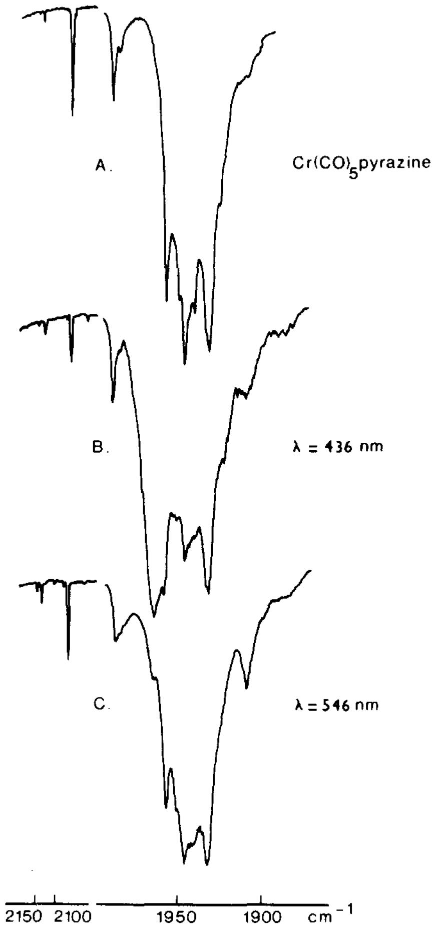

Figure 11. Infrared spectrum of $Cr(CO)_5$pyrazine in an Ar matrix at 10 K. A. After deposition. B. After 120 min photolysis with λ = 436 nm. C. After 120 min photolysis with λ = 546 nm.

Discussion

In order to understand the differences in photochemical behaviour between phosphorus and nitrogen donor complexes we have to consider both the UV–Visible absorption and photoelectron spectra of these compounds [21, 35]. When CO is replaced in $M(CO)_6$ by a ligand, the t_{2g} orbital is split into e (d_{xz}, d_{yz}) and b_2 (d_{xy}). The splitting will be mainly determined by a difference in π-interaction between CO and the ligand along the z-axis.

The σ-antibonding e_g orbital is also split into a_1 (d_{z^2}) and b_1 ($d_{x^2-y^2}$) respectively due to changes in σ-interaction. The relative positions of these two orbitals have been the subject of some controversy [2, 4, 34]. Recently with the aid of magnetic circular dichroism (MCD) spectra it was shown that the d_{z^2} is the lowest lying orbital [5]. In our laboratory a model, which takes into account both ligand field effects and electron repulsion parameters has been developed [36]. This model showed that the lowest excited state has predominant d_{z^2} character. From photoelectron spectra the energy difference between e and b_2 orbitals, $\Delta\pi$, in nitrogen donor complexes is found to be about 2.6 kK [21, 36]. A PES study of $M(CO)_5PX_3$ derivatives has shown, however, that the splitting of the e and b_2 orbitals can be neglected for these phosphorus donor complexes [35].

The energy difference between the d_{z^2} and $d_{x^2-y^2}$ orbitals ($\Delta\sigma$) can unfortunately only be estimated. With the assumption that the difference in energy between d_{xy} and $d_{x^2-y^2}$ hardly changes, when one CO in $Cr(CO)_6$ is replaced by another ligand, we can estimate the change of $\Delta\sigma$ going from $Cr(CO)_5PCl_3$ to $Cr(CO)_5$imine from the lowest LF transition in the absorption spectra (Table IV) and the energies of the filled d-orbitals deduced from the above mentioned photoelectron results. $\Delta\sigma$ appeared to increase by about 1 kK, when PCl_3 was substituted by an imine ligand. The same trend was found with the model of Daamen [36] in the series $C_5H_{11}N$, C_5H_5N, $P(C_6H_{11})_3$, $S(C_2H_5)_2$ and PCl_3 for $Cr(CO)_5L$ complexes.

It is now possible to understand the difference in photochemistry. Low energy photolysis of $Cr(CO)_5PCl_3$ will result in depopulation of the d_{xz}, d_{yz}, d_{xy} orbitals and in population of the σ-antibonding d_{z^2} orbital; cleavage of the Cr–P bond follows. Irradiation in higher energy bands of $Cr(CO)_5PCl_3$ will cause population of the σ antibonding $d_{x^2-y^2}$ orbital. Apparently a fast non radiative decay to d_{z^2} can then take place and again loss of PCl_3 is observed, as was also found for $W(CO)_5PCl_3$ [18].

Irradiation in low lying ligand field orbitals of $Cr(CO)_5$pyridine and $Cr(CO)_5$pyrazine will result in unique ligand rupture, but high energy irradiation will cause occupation of the $d_{x^2-y^2}$ orbital. This occupation leads to cleavage of the M–C bond resulting in *direct* formation of *cis*-$Cr(CO)_4$N-donor and not via a rearrangement of *trans*-$Cr(CO)_4$N into C_5 structure, as was one of the mechanisms suggested [7]. Apparently, contrary to the PCl_3 complex, fast non radiative decay from $d_{x^2-y^2}$ to d_{z^2} cannot occur for these nitrogen donor complexes. This result can be explained by the calculated increase of $\Delta\sigma$ between these orbitals going from the PCl_3 to the imine complexes.

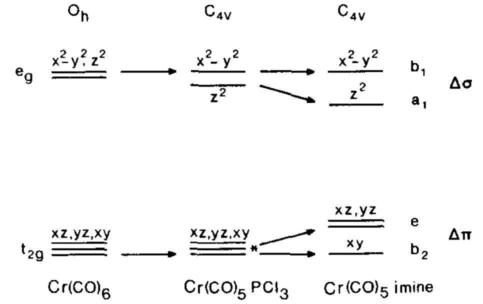

Scheme 1. Diagram of the d-orbitals, showing the relative magnitudes of the splittings going from $Cr(CO)_6$ to $Cr(CO)_5PCl_3$ and $Cr(CO)_5$imine. Apart from the observed splittings a destabilization of all orbitals occurs going from $Cr(CO)_5PCl_3$ to $Cr(CO)_5$pyridine and $Cr(CO)_5$pyrazine. Scheme 1 therefore, only presents the relative positions of these d-orbitals.

Influence of the Metal

It was already mentioned that the central metal atom has a large influence on the photochemistry [2, 7]. Tungsten derivatives of nitrogen donor complexes showed primarily M–N dissociation with much less M–C cleavage. In contrast with molybdenum and chromium complexes the tendency for CO rupture is increased at short wavelength photolysis. A sound explanation has not yet been found. In a note it was suggested that 313 and 366 nm excitation is not directed to the amine labilizing $^{1,3}E$ states for Cr-derivatives, as it is for Mo and W [7]. We do not agree with this expalanation since irradiation with 366 nm will result in tail absorption and occupation of a $^{1,3}E$ state of Cr-complexes, especially for $Cr(CO)_5$pyridine. Besides, the explanation does not elucidate the substantial low excitation of CO labilizing states, when photolyzing between roughly 200 and 350 nm, in which still W–N cleavage is the dominating process. We agree with the explanation that nonradiative decay probably increases going from Cr, Mo to W, due to spin–orbit coupling [7, 37].

Influence of the Ligand

The experiments have manifested that it is not possible to make the general statement that phosphorus donor ligands will always give M–P cleavage upon photolysis. It is now clear that the energy difference between the d_{z^2} and $d_{x^2-y^2}$ orbitals plays an important role. This difference depends on the σ

donor capacity of the ligand relative to CO. So, in the series PCl_3, PPh_3, pyridine this difference increased and both $M(CO)_5$ and *cis*-$M(CO)_4L$ complexes can be distinguished. On the other hand occupation of the σ-antibonding d_{z^2} orbital will not always result in M–L cleavage only, but also in M–C cleavage along the z-axis. For $M(CO)_5CS$ and $Mo(CO)_5PPh_3$ complexes both *cis* and *trans* derivatives were simultaneously found after photolysis indicating that as in $Cr(CO)_5$ these $M(CO)_4L$ molecules must have a C_{3v} structure in the excited state*.

Why this structure is not formed with nitrogen donor complexes and only the *cis* products are generated is not clear. Moreover, mixing of d_{z^2} and $d_{x^2-y^2}$ orbitals will make the observed photoprocesses more difficult to understand.

Mechanism of the Photoprocesses

In Scheme 2 the different photoprocesses are summarized. Photolysis of $M(CO)_5L$ results in an excited state after which photoproducts are distinguished. During the "reverse" reaction all product bands disappeared, simultaneously forming a *trans*-product. The question is now whether the product originates from $Cr(CO)_5$ or from *cis*-$Cr(CO)_4N$. If *trans*-$Cr(CO)_4N$ was produced from $Cr(CO)_5$ the following processes should have taken place:

We do not believe that this is possible for two reasons:

1. Photolysis of $Cr(CO)_5$ with $\lambda = 546$ nm generated from $Cr(CO)_6$ did not result in the appearance of $Cr(CO)_4$, but regenerated $Cr(CO)_6$.

2. Photolysis of $Cr(CO)_5N$ with $\lambda = 546$ nm during a long period did not produce any five coordinated species. Therefore, *trans*-$Cr(CO)_4N$ can only originate from *cis*-$Cr(CO)_4N$ via an excited state with C_{3v} symmetry.

$$\begin{array}{ccccc} cis\text{-}Cr(CO)_4N & \xrightarrow{546} & [Cr(CO)_4N]^* & \rightarrow & trans\text{-}Cr(CO)_4N \\ C_s & & C_{3v} & & C_{4v} \end{array}$$

Up till now, attempts to isomerize *trans*-$Cr(CO)_4N$ into *cis*-$Cr(CO)_4N$ failed.

Influence of the Medium

The photoreactions of $Cr(CO)_5$pyridine and $Cr(CO)_5$pyrazine in Ar matrices are closely related to the reactions in solution photochemistry. Unfortunately there are some contradictions: contrary to our results, Zink found for $W(CO)_5PCl_3$ very small W–P rupture [5, 18]. Furthermore, for $W(CO)_5CS$ the formation of $W(CO)_4CS$ occurred with very low efficiency, while Poliakoff did not detect CS rupture [5, 14]. We do not know what is the reason for this contradiction. From a study of $M(CO)_6$ molecules in matrices it was concluded that matrices can influence the structure ($M(CO)_6$: $O_h \rightarrow D_{2h}$) [8] and it

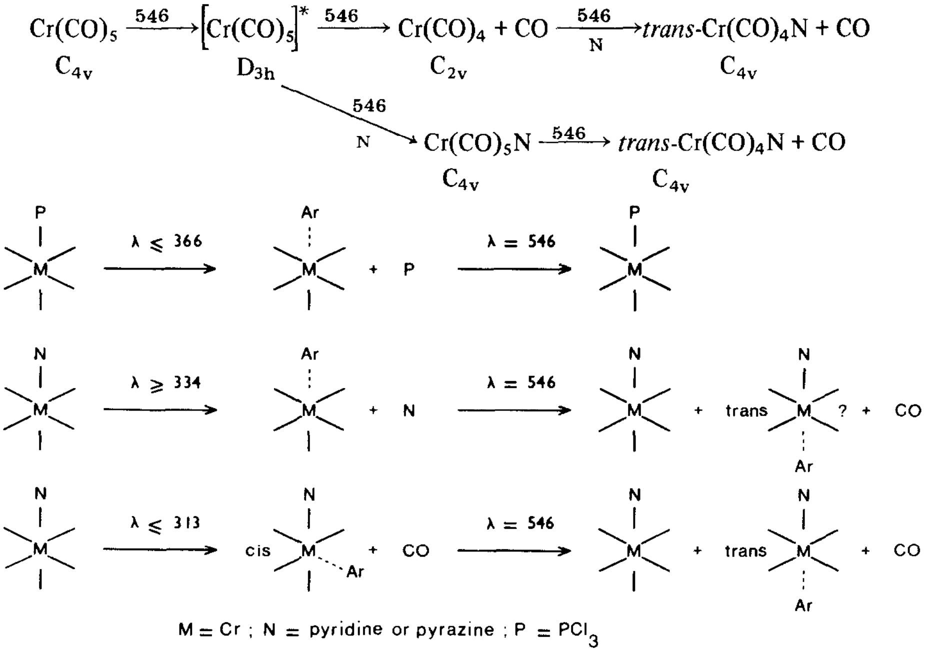

Scheme 2. The influence of the ligand upon photolysis with various wavelengths.

---

*It was suggested that, because of the smaller difference between CO and PPh_3 compared to CO and pyridine, both *cis*- and *trans*-complexes were observed. However, in $M(CO)_5$-PCl_3 complexes this difference between CO and the unique ligand is decreased extensively and even then no significant *trans*-complex formation was detected.

is possible that the matrix favours one of the possible structures in the excited state. It is therefore necessary that more $M(CO)_5L$ complexes are studied in various matrices. Besides this it is of great importance to know what the exact positions of all LF transitions are, since most transitions are obscured by charge transfer bands. With the help of magnetic circular dichroism spectra, however, these transitions may be determined for this type of complexes.

Conclusions

Matrix photochemistry of $Cr(CO)_5PCl_3$, $Cr(CO)_5$-pyridine and $Cr(CO)_5$pyrazine has shown that the unique ligand strongly influences the photochemical behaviour of these complexes. Although little is known about conversion processes of $M(CO)_5L$ compounds, the photochemical results clearly indicate that the speed of nonradiative decay between $d_{x^2-y^2}$ and d_{z^2} orbitals, is strongly affected by the type of unique ligand.

This conclusion is confirmed by the result, estimated from photoelectron and absorption spectral data, that the difference in energy between $d_{x^2-y^2}$ and d_{z^2} increases going from the PCl_3 to the pyridine and pyrazine complexes.

Matrix isolation spectroscopy has again shown to be an important tool for the determination of intermediates in photochemical processes, although it is disappointing that these processes are not always related to solution photochemistry. Therefore, it is necessary that far more complexes are studied by matrix isolation spectroscopy.

Acknowledgements

The authors express their thanks to H. Luyten, B. H. Klein Meulekamp and G. C. Schoemaker for their technical assistance throughout these studies and Drs. H. Daamen is thanked for preparing the $Cr(CO)_5$-imine complexes.

References

1 M. Wrighton, G. S. Hammond and H. B. Gray, *Mol. Photochem., 5,* 179 (1973).
2 M. Wrighton, *Inorg. Chem., 13,* 905 (1974).
3 M. Wrighton, *Chem. Rev., 74,* 401 (1974).
4 M. Wrighton, H. B. Abrahamson and D. L. Morse, *J. Am. Chem. Soc., 98,* 4105 (1976).
5 R. M. Dahlgren and J. I. Zink, *Inorg. Chem., 16,* 3154 (1977).
6 D. J. Darensbourg and M. A. Murphy, *J. Am. Chem. Soc., 100,* 463 (1978).
7 D. J. Darensbourg and M. A. Murphy, *Inorg. Chem., 17,* 884 (1978).
8 M. A. Graham, M. Poliakoff and J. J. Turner, *J. Chem. Soc. A,* 2939 (1971).
9 R. N. Perutz and J. J. Turner, *Inorg. Chem., 14,* 262 (1975).
10 R. N. Perutz and J. J. Turner, *J. Am. Chem. Soc., 97,* 4791 (1975).
11 R. N. Perutz and J. J. Turner, *J. Am. Chem. Soc.,97,* 4800 (1975).
12 J. K. Burdett, M. A. Graham, R. N. Perutz, M. Poliakoff, A. J. Rest, J. J. Turner and R. F. Turner, *J. Am. Chem. Soc., 97,* 4805 (1975).
13 M. Poliakoff, *Inorg. Chem., 15,* 2022 (1976).
14 M. Poliakoff, *Inorg. Chem., 15,* 2892 (1976).
15 J. D. Black and P. S. Braterman, *J. Organomet. Chem., 63,* C19 (1973).
16 A. J. Rest and J. R. Sodeau, *Chem. Comm.,* 696 (1975).
17 T. M. McHugh, A. J. Rest and J. R. Sodeau, *J. Chem. Soc. Dalton,* accepted for publication.
18 G. Boxhoorn and A. Oskam, *Inorg. Chim. Acta, 29,* 243 (1978).
19 G. Boxhoorn and A. Oskam, *Inorg. Chim. Acta, 29,* L207 (1978).
20 W. Strohmeier and F. J. Muller, *Chem. Ber., 102,* 3608 (1969).
21 H. Daamen and A. Oskam, *Inorg. Chim. Acta, 27,* 209 (1978).
22 R. Poilblanc and M. Bigorgne, *Bull. Soc. Chim. Fr., 29,* 1301 (1962).
23 G. Boxhoorn, A. C. Jesse, J. M. Ernsting and A. Oskam, *Thermochim. Acta, 27,* 261 (1978).
24 M. M. Rochkind, *Science, 160,* 197 (1968).
25 R. N. Perutz and J. J. Turner, *J. Chem. Soc. Faraday Trans. II, 69,* 452 (1973).
26 W. M. Adams, "Metal–Ligand and Related Vibrations", Edward Arnold, London (1967).
27 D. J. Darensbourg and T. L. Brown, *Inorg. Chem., 7,* 959 (1968).
28 G. R. Dobson, *Adv. Inorg. Chem. and Radiochem., 8,* 1 (1966).
29 F. R. Young, R. A. Levenson, M. N. Memering and G. R. Dobson, *Inorg. Chim. Acta, 8,* 61 (1974).
30 C. Jeanne, R. Prince and R. Poilblanc, *Spectrochim. Acta, 31A,* 819 (1975).
31 M. A. M. Meester, R. C. J. Vriends, D. J. Stufkens and K. Vrieze, *Inorg. Chim. Acta, 19,* 95 (1976).
32 G. Boxhoorn, D. J. Stufkens and A. Oskam, unpublished results.
33 H. Daamen, D. J. Stufkens and A. Oskam, unpublished results.
34 F. A. Cotton, W. T. Edwards, F. C. Rauch, M. A. Graham, R. N. Perutz and J. J. Turner, *J. Coord. Chem., 2,* 247 (1973).
35 H. Daamen, G. Boxhoorn and A. Oskam, *Inorg. Chim. Acta 28,* 263 (1978).
36 H. Daamen, D. J. Stufkens and A. Oskam, *Inorg. Chim. Acta, 32,* 249 (1979).
37 A. W. Adamson and P. D. Fleischauer, "Concepts of Inorganic Photochemistry", Wiley, New York (1975).